Singularity Robust Motion and Force Control in Operational Space: A Canopy Polishing Application

Marcelo H. Ang Jr.
Department of Mechanical Engineering
National University of Singapore
Singapore 119260

Denny Oetomo, Rodrigo Jamisola Jr.
Department of Mechanical Engineering
National University of Singapore
Singapore 119260

Oussama Khatib
Department of Computer Science
Stanford University
CA 94305

S.Y.Lim
Gintic Institute
of Manufacturing Technology
Singapore 638075

Abstract

A singularity handling algorithm is proposed to allow a manipulator to move through singular configurations in a stable manner, while performing motion and force control tasks. This algorithm is developed in Operational Space Framework and addresses the problem of finding the inverse of a singular Jacobian matrix by identifying and removing the singular component(s) of motion. The method was applied to a PUMA manipulator on a polishing task involving motion and force control. The experimental results obtained from this implementation illustrate the effectiveness of the approach.

1 Introduction

Simultaneous motion and force control of robotic manipulators can be achieved using the operational space approach [1], as opposed to the traditional joint-space methods involving inverse kinematics and joint space dynamics. The operational space approach controls motion of the robot's end-effector by applying a virtual force to bring the end-effector to the goal position. In force control, the desired forces are used directly and combined with the virtual forces to compute an operational space force required to drive the robot. The operational space force is achieved by the joint actuators by taking into account the manipulator's dynamic parameters as seen from the robot's end-effector. Tedious inverse kinematics of position algorithms are therefore not needed. The operational space approach therefore provides a natural and unified force and motion control approach in the operational or task (end-effector) space of the robot. The formulation is applicable to redundant robots whose number of joints exceeds those required by the task. Since the control is done in the operational space, the end-effector control is decoupled from null-space control and the redundant joints can be controlled independently without affecting the end-effetor's motion or ability to exert forces [2].

It is well-known that singularities inherently limit the manipulator's motion and force capabilities. In the operational space approach, the operational force may not be realized if the manipulator is at a singular configuration. Many methods have been proposed to handle singularities. Some attempts to avoid it [3] [4], and some to go through it gracefully [5][6][7][8]. However, most kinematics-based methods only work in handling singularities in motion control. Relatively fewer works have been reported on how singularities are handled in force control tasks, or in tasks involving both motion and force control.

This paper presents the results of our practical implementation of the operational space approach with some improvements in making the approach robust to singularities. We consider the task of polishing an aircraft canopy of unknown geometry (Figure 1). This is a similar task to the one performed in [9], although in that experiment, the robot learnt the geometry of the canopy before executing the task (as compared to our experiment where geometry stays unknown). The PUMA 560 robot holds a polishing tool and is commanded to exert a normal force of 20 N while executing a polishing motion that is tangential to the surface. The PUMA robot is mounted on a mobile base whose motion is controlled independently using a joystick by the operator. The base motion provides the needed workspace and is not known by the robot. Our compliant motion control strategy allows the unified force and motion control in spite of unknown motions of the base and unknown geometry of the canopy.

In the next section, we review the operational space formulation. We then present details on how singularities are handled and integration into the operational space formulation. In Section 5, we present implementation details for the canopy polishing application and show results.

Figure 1: The experimental setup showing PUMA maintaining a constant force over wrist singularity.

2 Operational Space Formulation

The Operational Space Formulation [1] is a control approach where the desired motion and contact forces are achieved by computing an operational space force F (expressed in operational space, or Cartesian space as seen from the end-effector or tool) that would drive the end-effector to the desired motion and contact forces. The operational space force is a combination of the force for free motion control and force for constrained motion (force control). It is then converted to joint actuator commands by

$$\begin{array}{c} \Gamma = J^T F + \mathcal{N}^T \Gamma_0 \\ \mathcal{N} = [I - \bar{J} J] \end{array} \quad (1)$$

where Γ is the joint actuator values, J is the manipulator Jacobian in operational space, and $\mathcal{N}$ is the null space of J^T. Γ_0 is used to control the null motions. $\bar{J}$ is an inverse of the Jacobian matrix, where in this case the *dynamically consistent inverse* is used so motion in the null space would not have any contribution to the forces at the end effector [10].

Free motion, in Operational Space Formulation, is generated by a virtual force vector $\mathbf{F}^*_{motion}$ that would bring the end-effector from its current position $\mathbf{x}$ to the desired position $\mathbf{x}_d$.

$$\mathbf{F}^*_{motion} = \mathbf{I}\ddot{\mathbf{x}}_d - \mathbf{k}_{vmotion}(\dot{\mathbf{x}} - \dot{\mathbf{x}}_d) - \mathbf{k}_{pmotion}(\mathbf{x} - \mathbf{x}_d) \quad (2)$$

The dynamics of the manipulator as seen from the end-effector is then utilized to compute the operational force $\mathbf{F}_{motion}$:

$$\mathbf{F}_{motion} = \hat{\Lambda}(x)\mathbf{F}^*_{motion} + \hat{\boldsymbol{\mu}}(x, \dot{x}) + \hat{\mathbf{p}}(x) \quad (3)$$

where $\hat{\Lambda}$ is the inertia matrix, $\hat{\mu}$ is the Coriolis and centrifugal forces, and $\hat{p}$ is gravitational vector, all in operational space:

$$\begin{array}{rcl} \hat{\Lambda}(x) & = & [J(q)\hat{A}(q)J^T(q)]^{-1} \\ \hat{\mu}(x\dot{x}) & = & [J^{-T}(q)\hat{B}(q) - \Lambda(q)\hat{H}(q)][\dot{q}\dot{q}] \\ \hat{p}(x) & = & J^{-T}(q)\hat{g}(q) \end{array} \quad (4)$$

$J(q)$ is the Jacobian matrix, $\hat{A}$ is the joint space inertia matrix, $\hat{B}(q)[\dot{q}\dot{q}]$ is the joint space Coriolis and centrifugal matrix, $\hat{H}(q)$ is obtained from $\hat{H}(q)[\dot{q}\dot{q}] = \dot{J}(q)\dot{q}$, and $\hat{g}$ is the joint space gravitational vector. All the " ˆ " signifies modelled parameters as opposed to the actual dynamic properties of the manipulator.

The control is similar to the well-known computed-torque control [11] where the control algorithm results in a unit mass system. Here, the computed-torque control approach is applied in operational space.

In force control applications, the operational space force $\mathbf{F}_{force}$ required at the end-effector is

$$\mathbf{F}_{force} = \hat{\Lambda}(x)\mathbf{F}^*_{force} + \hat{\boldsymbol{\mu}}(\mathbf{x}, \dot{\mathbf{x}}) + \hat{\mathbf{p}}(x) + \mathbf{F}_{contact} \quad (5)$$

where,

$$\mathbf{F}^*_{force} = \mathbf{k}_{pforce}(\mathbf{F}_d - \mathbf{F}_{contact}) + \mathbf{k}_{iforce} \sum (\mathbf{F}_d - \mathbf{F}_{contact}). \quad (6)$$

is the control law and $\mathbf{F}_{contact}$ is the force exerted on the environment and is related to the force sensor reading, $\mathbf{F}_{sensor}$, by

$$\mathbf{F}_{contact} = -\mathbf{F}_{sensor} \quad (7)$$

In operational space, the robot end-effector has six degrees of freedom and these degrees of freedom has to be partitioned into motion control and force control spaces. The partitioning is done via selection matrices [1].

The generalized *task specification matrices* Ω is then defined as

$$\Omega = \begin{pmatrix} S^T_{Tool}\Sigma_{\mathcal{F}}S_{Tool} & 0 \\ 0 & S^T_{Tool}\Sigma_{\mathcal{M}}S_{Tool} \end{pmatrix} \quad (8)$$

where $\Sigma_{\mathcal{F}}$ and $\Sigma_{\mathcal{M}}$ are diagonal matrices that contains binary values where "1" signifies application of motion control and "0" force control. $\bar{\Omega}$ is obtained using $\bar{\Sigma}_{\mathcal{F}}$ and $\bar{\Sigma}_{\mathcal{M}}$ which are the complements of $\Sigma_{\mathcal{F}}$ and $\Sigma_{\mathcal{M}}$.

Ω and $\bar{\Omega}$ are then applied to the $\mathbf{F}_{motion}$ and $\mathbf{F}_{force}$, respectively in Equations (3) and (5). The unified force and motion control is then achieved by adding the operational forces for motion and force control, resulting in:

$$\mathbf{F} = \mathbf{F}_{motion} + \mathbf{F}_{force} \tag{9}$$

where

$$\mathbf{F}_{motion} = \hat{\Lambda}(x)\Omega\mathbf{F}^*_{motion} + \hat{\boldsymbol{\mu}}(x,\vartheta) + \hat{\mathbf{p}}(x) \tag{10}$$

and

$$\mathbf{F}_{force} = \hat{\Lambda}(x)\bar{\Omega}\mathbf{F}^*_{force} + \mathbf{F}_{sensor}. \tag{11}$$

Note that the Coriolis, centrifugal and gravity forces are only applied once in the unified force and motion control.

When $\mathbf{F}_{motion}$ and $\mathbf{F}_{force}$ are obtained, the combined $\mathbf{F}$ is sent as torque by Equation 1.

3 Singularity Robust Operational Space Formulation

A manipulator is considered singular when it loses one or more degrees of freedom. At the singular configuration, the manipulator Jacobian is rank deficient.

In Nakamura [8] and Hsu [3], redundant motion was utilized to follow a potential function that maximizes the manipulability of the robot, hence avoiding singular configuration (where manipulability is zero). A measure of manipulability is presented in [12]. Chiaverini and Egeland [7] also identified and removed the degenerate components of motion, and applied pseudo inverse with the collapsed Jacobian in the kinematics-based approach. Null space was also utilised to avoid excessive joint rate in the vicinity of singularity, caused by the aligning of two or more axes of joint rotation. Cheng [6] performed an analysis and handling on PUMA 560 also by releasing the exactness in the singular direction and providing the extra redundancy to the achievable direction. Their *Compact QP method* would then attempt to minimize the tracking error in singular direction. Kircanski [13] utilises the Singular Value Decomposition (SVD) and replaces the zero value at the diagonal matrix at singularity with a continuous function of non-zero value.

To be able to handle singularities robustly, we need to know the motion limitations of the manipulator at each singular configuration. Since a row of the Jacobian indicates the corresponding direction of the task-space degree of freedom, when a manipulator loses a degree of freedom, a row of the Jacobian will then be zero. The key strategy is the required kinematic transformation of the Jacobian to make one row zero. The transformation involves moving the velocity point of interest of the end-effector and expressing the velocity in an appropriate Cartesian frame. After transformation, the row of zeros represents the axis direction that is degenerate. The row of zeros means no velocity in joint space could produce the DOF in task space.

The idea we adopt is to identify and remove these degenerate components as motivated by Chiaverini's work [7]. In the vicinity of the singularity, a region is defined as the singular region, where the row(s) of zeros in the Jacobian is then removed, therefore collapsing the Jacobian into full rank. In our approach, however, we treat the manipulator as momentarily redundant with respect to the task and we use the dynamically consistent inverse to ensure decoupling of null space from the end-effector space . Removing the row results in a subspace of the operational space that is orthogonal to the direction of singularity. As shown later, we employ null motion strategies to achieve tasks in spite of singularities.

The operational space force $\mathbf{F}$ in Eq. (9) that achieves the unified force and motion control and the Jacobian are first transformed into the appropriate identified frame where at least one row of the Jacobian is zero. The degenerate axis direction(s) is then removed resulting in less DOF in task space. Operational space control (1) is then applied to the system with Γ_0 formulated to realize the desired null motion. Since the task has been momentarily reduced to a lower DOF, the task in the degenerate direction that has been removed is no longer possible. If the desired task is away from the degenerate direction, then there is no problem, and desired task can be achieved.

If the desired task is along the degenerate direction, null space motions are then utilized. Singularities could be categorized into type 1 and type 2 singularities [14] based on the effects of null space torques Γ_0 . Type 1 is when the null space torques creates end-effector motion/forces only in the singular direction(s). Null space motion is not supposed to create any effect on the end-effector. In this case, null space motion creates motion along the singular direction because the singular direction is no longer part of the task, and forces/motion resulting from null space torques are only decoupled from the remaining DOF of the end-effector. Type 2 is when the singular directions are changed by null-space torques without affecting the end-effector motion/forces. Γ_0 is formulated to be the gradient descent of a potential function that is minimum at a desired joint configuration (for type 1 singularities) or at a direction orthogonal to the degenerate direction (for type 2 singularities). The desired task is then realized. Once the manipulator is out of the singular region, the task DOF are fully restored and control takes place with the full Jacobian. The null torques may affect the ability for the end-effector to track time-dependent trajectories. Hence path planning approaches may be needed to keep the singular directions orthogonal to end-effector motion/forces in the neighborhood of singularities.

4 Application to The PUMA 560

4.1 Identifying Singularities and Singular Directions

To simplify the identification of singularities, the control reference point of the manipulator is transformed to the center of the spherical wrist. This is often done for anthropomorphic arm to decouple the position control so that it is only affected by the first three joints of the robot. Orientation, however is still affected by all six joints. The decoupled Jacobian will be in the form of: $J_d = MJ$ where

$$J_d = \begin{bmatrix} J_{11} & 0_{3x3} \\ J_{21} & J_{22} \end{bmatrix} \tag{12}$$

J_d is the decoupled Jacobian and M is a transformation matrix to transform the operational point from the end effector point (tool tip) to the wrist point. However, the determinant of the transformation matrix M is 1 [6], therefore

$$Det(J_d) = Det(M)Det(J) \tag{13}$$

In the case of PUMA, which is a 6 DOF manipulator, the Jacobian is a square matrix. This simplifies the identification process to be

$$Det(J) = Det(J_d) = Det(J_{11})Det(J_{22}) \tag{14}$$

Solving for the determinants of the 3 by 3 matrices of J_{11} and J_{22}, the determinant of the Jacobian for PUMA is

$$\begin{aligned} &Det(J_{11}) = -a_2(d_4C_3 - a_3S_3)(d_4S_23 + a_2C_2 + a_3C_23) \\ &Det(J_{22}) = -S_5 \end{aligned} \tag{15}$$

where the singularities generated from J_{11} are called position singularities, and that from J_{22} orientation singularity. The PUMA 560 robot therefore has three singularities, corresponding to:
wrist: $S_5 = 0$
elbow: $d_4C_3 - a_3S_3 = 0$
head: $d_4S_23 + a_2C_2 + a_3C_23 = 0$
The frame assignment on PUMA is shown in Figure 2. The modified D-H parameters can be found in [15]

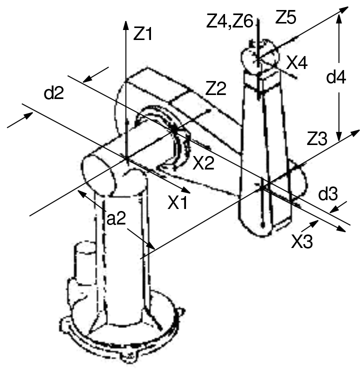

Figure 2: PUMA and the frame assignment used in the experiment, where a_2=0.43m, a_3=-0.0203m, d_2=0.2435m, d_3=-0.0934m, and d_4=0.4331m

From observation, the degenerate direction of head singularity is the translation along Y-axis of Frame{1}. For elbow singularity, it is the translation along the line that connects the origin of Frame{1} to the wrist point (Frames 4, 5, 6). For the wrist singularity, it is the rotation around the X-axis of Frame{4}.

4.2 Head Singularity

For the head singularity, the manipulator loses the translation DOF along Y-axis of Frame{1}. The Jacobian is therefore transformed to Frame{1}. Equation 16 shows the top half of the Jacobian in Frame{1}. As shown in Equation 15, $(d_4S_23 + a_2C_2 + a_3C_23) = 0$ at Head singularity, therefore setting all the values on the second row of Jacobian ${}^1J$ to zero. The last three column of the top half of the Jacobian is a 3 by 3 zero matrix (as shown in 12)
${}^1J_{11} =$

$$\begin{pmatrix} -d_2 - d_3 & d_4C_{23} - a_2S_2 - a_3S_{23} & d_4C_{23} - a_3S_{23} \\ a_2C_2 + a_3C_{23} + d_4S_{23} & 0 & 0 \\ 0 & -a_2C_2 - a_3C_{23} - d_4S_{23} & -a_3S_{23} - d_4S_{23} \end{pmatrix} \tag{16}$$

The second row is removed and the Jacobian collapses to a 5 by 6 matrix. $\mathbf{F}_{motion}$ and $\mathbf{F}_{force}$ are then transformed to the same frame (Frame {1}). The dynamic parameters required for the generation of $\mathbf{F}_{motion}$ and $\mathbf{F}_{force}$ as in Equation 4 are calculated from this collapsed Jacobian.

This is a type 2 singularity because null space torques can change the singular directions by moving joint 1. Consider the desired task to be a motion/force task along the Y-axis of Frame{1} and the robot is at the head singularity configuration. It is desired to shift the singular direction to be along the X-axis of Frame{1}. The following potential function on joint 1 achieves this:

$$V(q_1) = k_N(q_1 - q_{1desired})) \tag{17}$$

where k_N is the constant gain, $q_{1desired}$ is $90^o sgn(^1F_Y)$, and $sgn(^1F_Y)$ is the sign of the desired force in the degenerate direction (along the positive or the negative Y-axis of Frame{1}).

This potential function is minimized when the singular direction is orthogonal to the desired task. Γ_0 is then

$$\Gamma_0 = \nabla V(q) = 2k_N(q_1 - q_{1desired})) \tag{18}$$

4.3 Elbow Singularity

The degenerate direction for elbow singularity is the line connecting the origin of the Base Frame with the wrist point. Let Frame{B} be the frame whose X-axis is along the line connecting the origin of the Base Frame with the wrist point (Figure 3). Frame{B} is obtained by rotating Frame{2} by angle $-\beta$, around its Y-axis (Figure 2). β is defined as:

$$\beta = Tan^{-1}\left[\frac{d_2 + d_3}{a_2 + a_3C_3 + d_4S_3}\right] \tag{19}$$

The direction of singularity is the translation along X-axis of Frame{B}. The Jacobian is transformed to Frame{B}. The elements of the first row of the Jacobian in Frame{B} is

$^BJ[1][1] = \frac{(d_2+d_3)S_2(d_4C_3-a_3S_3)}{(a_2+a_3C_3+d_4S_3)D}$

$^BJ[1][2] = \frac{(d_4C_3-a_3S_3)(a_2+a_3C_3+d_4S_3)^2 D}{a_2^2+d_2^2+2d_2d_3+d_3^2+2a_2a_3C_3+a_3^2C_3^2+2a_2d_4S_3+d_4^2S_3^2+a_3d_4Sin[2q3]}$

$^BJ[1][3] = \frac{d_4C_3-a_3S_3}{D}$

where: $D = \sqrt{1 + \frac{(d_2+d_3)^2}{(a_2+a_3C_3+d_4S_3)^2}}$

At the elbow singularity, $(d_4C_3 - a_3S_3) = 0$ and the first row of $^BJ_{11}$ is a zero row ($^BJ[1][1] =^B J[1][2] =^B J[1][3] = 0$). This shows that the singular (degenerate) direction lies along the X-axis of Frame{B} (Figure 3). The rest of the procedure in removing the singular component is the same as that of head singularity.

This is a type 1 singularity because null space torques creates motion in the degenerate direction.

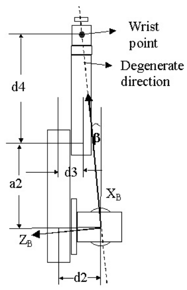

Figure 3: Degenerate direction in elbow singularity

Consider the desired task to be a motion/force from elbow straight to elbow up position. It is desired to set a potential function on joint 3 to move from $q_3 = 90^o$ to $q_3 = 135^o$ (see definition of joint 3 in Figure 2). The potential function is:

$$V(q_3) = k_N(q_3 - (q_{3desired})) \tag{20}$$

where $q_{3desired}$ is 135^o for elbow up position.

4.4 Wrist Singularity

In wrist singularity, there is no entire row of the Jacobian that is zero. The lower half of the decoupled Jacobian when expressed in $Frame\{4\}$ is (due to space constraint, it is split into $^4J_{21}$ and $^4J_{22}$ as defined in Eq. 12)

$$^4J_{21} = \begin{pmatrix} -C_4S_{23} & S_4 & S_4 \\ S_{23}S_4 & C_4 & C_4 \\ C_{23} & 0 & 0 \end{pmatrix}$$

$$^4J_{22} = \begin{pmatrix} 0 & 0 & S_5 \\ 0 & 1 & 0 \\ 1 & 0 & C_5 \end{pmatrix} \tag{22}$$

The wrist singularity is caused by the matrix $^4J_{22}$ going rank-deficient. This is when $\vartheta_5 = 0$, and the first row of $^4J_{22}$ becomes a zero row. Because $Det(J) = Det(J_{11})Det(J_{22})$ in (15), a rank-deficient $^4J_{22}$ would cause the robot to be singular.

It can be argued however, that at wrist singularity, rotational motion around X-axis of $Frame\{4\}$ is still possible, because there are still non-zero components from the first row of $^4J_{21}$. The motion is possible, but it would be generated by the first three joints of the robot, thus changing the position. Therefore it would not be able to maintain a certain position and achieve the rotation around X-axis of $Frame\{4\}$ at the same time.

This is a type 2 singularity. If the rotation around X-axis of Frame{4} is needed when the manipulator is in wrist singularity, null space motion can be applied to joint 4 to shift the degenerate direction orthogonal to the desired path. The potential function used is:

$$V(q_4) = k_N(q_4 - (q_{4desired})) \tag{23}$$

where $q_{4desired}$ is $90^o sgn(^4M_X)$, where $sgn(^4M_X)$ is the direction of moment around the X-axis of Frame{4} desired to achieve the task (which is the degenerate direction).

Once the null space motion rotates joint 4 to be out of singular region, the 6 DOF motion and force control will be in place again.

The wrist singularity is the most common in PUMA arm, and the performance of the PUMA polishing the canopy while going through this singularity is presented and compared to that of non-singular motion.

5 Canopy Polishing Application

Our singularity-robust unified force and motion control was implemented with the experiment setup as shown in Figure 1. The task is to polish an aircraft canopy (of an F-5 fighter) with an unknown geometry. The PUMA manipulator was to maintain a force of 20N and sinusoidal (with respect to time) motion tangential to the unknown surface while moving across the wrist singularity. The force direction is along Z-axis and the motion direction is along X-axis of the tool frame. Force control is also applied to maintain zero moment around the X and Y axes of Tool Frame. This creates the compliant behaviour so that the tool would keep itself perpendicular to the surface of the canopy.

The null motion required in escaping the wrist singularity is the rotation around the Z-axis of joint 4 (see Figure 4). The potential function is constructed by

$$V(q_4) = k_N(M_X Sign(M_Y) - M_{XDes})^2 \tag{24}$$

where k_N is a constant gain, M_X and M_Y are the moment around the X and Y axes of the Tool Frame, as read by the force torque sensor, $M_X D$ is the desired moment, which is set to zero. $Sign(M_Y)$ is included to select the direction of null space torque applied to joint 4 by taking into account the moment generated by gradient of the unknown surface around Y-axis of the Tool Frame.

The PUMA manipulator is mounted on a mobile base which is operator-controlled via a joystick. The operator moves the base to provided the extended workspace to cover the entire canopy. The base motion is not known to the robot and is treated as a disturbance. The dynamic model of PUMA 560 is obtained from [15]. The complete dynamic model was employed except static friction is not modelled. We implement the control laws with a servo rate of 1 KHz. A six-axis force/torque sensor is mounted between the end-effector and polishing tool.

The result of the unified motion and force control is shown in Figure 5.

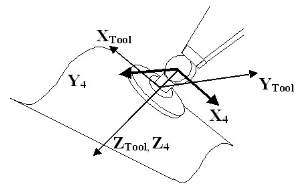

Figure 4: PUMA wrist at singularity, where Z axes of Tool Frame and $Frame\{4\}$ are aligned. The lost DOF is the rotation around X-axes of $Frame\{4\}$

Experimental results are shown in Figure 5. The top graph shows the position error in X and Y axis of the tool frame (for Tool Frame assignment, see Figure 4). Motion executed was a path along the X-axis of the Tool Frame (Figure 4), with a sinusoidal displacement with respect to time. The error in X direction is mainly due to the unmodelled friction between the grinder tool and the canopy surface. There was not much motion in Y-direction, as the task was set to maintain constant Y (straight line). The middle graph shows the force applied perpendicular to the canopy surface. This is along the Z-axis of of the manipulator tool frame. The bottom graph shows the determinant value of the Jacobian, showing the points where the wrist was at singularity $Det(J) = 0$.

The result of the experiment shows that it is possible for the manipulator to move across singularity while maintaining its performance on motion and force control. It was expected that some error might be introduced by the switching of control as the manipulator crosses into and out of the singular region. However, the experimental data does not show a statistically significant correlation between the singularity and deterioration in performance.

Compared to the case where the manipulator does not go through singular configurations, the performance does not appear to be any significantly worse. The force performance for this particular set of experimental data is 19.99N (average) with 0.8N standard deviation when polishing along a path through singularity and is 20.0N (average) with 0.7N standard deviation in a non-singular path. The average position error is 0.0008m with 0.006m standard deviation in

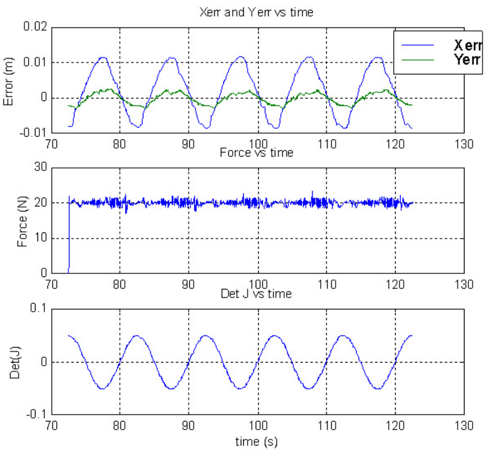

Figure 5: Result of Experiment

non-singular motion. In our experiment, the average position error for X is 0.002m with 0.007m standard deviation while Y is 0.0002m with 0.002m standard deviation. The error was periodic due to the sinusoidal pattern of the trajectory with respect to time.

6 Conclusion

The results of this experiment showed the feasibility of unified force and motion control through singular region using our proposed approach. Motion and force control errors while tracing a path through the singular region were found to be not significantly larger than those while moving through non-singular paths. The result is not only a more stable system, but also a better usage of the workspace of the robot, as it can move through the singular region rather than avoiding it.

References

[1] Oussama Khatib, "A unified approach for motion and force control of robot manipulators: The operational space formulation," *IEEE J. Robotics and Automation*, vol. RA-3, no. 1, pp. 43–53, 1987.

[2] Oussama Khatib, "Motion/force redundancy of manipulators," *Proc, Japan-USA Symposium on Flexible Automation, Kyoto Japan*, pp. 337–342, 1990.

[3] P. Hsu, J. Hauser, and S. Sastry, "Dynamic control of redundant manipulators," *IEEE Intl. Conf. Robotics and Automation*, vol. 1, pp. 183–187, 1988.

[4] Tsuneo Yoshikawa, "Analysis and control of robot manipulators with redundancy," in *Robotics Research*, M. Brady and R. Paul, Eds., pp. 735–747. MIT Press, Cambridge, MA, 1984.

[5] E. W. Aboaf and R. P. Paul, "Living with the singularity of robot wrists," *IEEE Intl. Conf. for Robotics and Automation*, pp. 1713–1717, 1987.

[6] Fan-Tien Cheng, Tzung Liang Hour, York-Yin Sun, and Tsing-Hua Chen, "Study and resolution of singularities for a 6-dof puma manipulator," *IEEE Trans. Systems, Man and Cybernetics*, vol. 27 2, pp. 332–343, 1997, Part B.

[7] S. Chiaverini and O. Egeland, "A solution to the singularity problem for six-joint manipulators," *Proc. IEEE for Robotics and Automation*, vol. 1, pp. 644–649, 1990.

[8] Y. Nakamura and H. Hanafusa, "Inverse kinematics solutions with singularity robustness for robot manipulator control," *ASME J. of Dynamic Systems, Measurement, and Control*, vol. 108, pp. 163–171, 1986.

[9] George A. Grabits, "Polishing aerospace transparencies," *Conference of Robotic Solutions in Aerospace Manufacturing*, pp. MS86–203 1–22, March 1986, Orlando, Florida.

[10] K. Chang and O. Khatib, "Manipulator control at kinematic singularities: A dynamically consistent strategy," *Proc. IEEE/RSJ Int. Conference on Intelligent Robots and Systems*, vol. 3, pp. 84–88, 1995.

[11] J. Y. S. Luh, M. W. Walker, and R. P. Paul, "Resolved-acceleration control of mechanical manipulators," *IEEE Transactions on Automatic Control*, vol. 25, no. 3, pp. 468–474, 1980.

[12] Tsuneo Yoshikawa, "Manipulability of robotic mechanisms," *Intl. J. Robotics Research*, vol. 4, no. 2, pp. 3–9, Summer 1985.

[13] Manja V. Kircanski, "Symbolical singular value decomposition for a 7-dof manipulator and its application to robot control," *IEEE Conf. on Robotics and Automation*, vol. 3, pp. 895–900, 1993.

[14] Oussama Khatib, "Advanced robotics," Lecture Notes, 1996, Stanford University.

[15] J. Burdick B. Armstrong, O. Khatib, "The explicit dynamic model and inertial parameters of the puma 560 arm," *IEEE Intl. Conf. Robotics and Automation*, pp. 510–518, 1986.